

# Transient laminar flow in hydraulic networks based on a semi-analytical impulse response method

A. Jarquin Laguna, A. Tsouvalas

Delft University of Technology, the Netherlands

The importance of transient analysis in hydraulic networks has been well recognized due to abrupt changes in flow or pressure introduced by valve closures or component failures. Therefore, accurate and robust numerical models are necessary to analyse the travelling pressure waves as a result of such sudden changes. This paper presents the formulation of a semi-analytical impulse response method applied to transient laminar flow in hydraulic networks. The method is based on the exact solution of a two-dimensional viscous model in the frequency domain with various interface and boundary conditions. The numerical computation is based on the use of the fast Fourier transform and the discrete numerical convolution with respect to time. To illustrate the method, a numerical example is presented and the results are compared with the method of modal approximations that is widely used in practice. The results show that the proposed method is able to predict the transient behaviour with better accuracy and without the need of spatial discretization. Thus, it is expected that for large networks, the computational cost of the impulse response method will have a great advantage when compared to existing grid-space methods.

*Key words: Transient laminar flow, hydraulic networks, impulse response method*

## 1 Introduction

Transient flow in hydraulic networks is a common phenomenon as a result of either accidental or normal operation of hydraulic systems. The study and analysis of unsteady-flow conditions is very important due to the large disturbances in pressure and flow conditions that might be introduced [1]. Several numerical methods exist to model fluid transients [2, 3]. To date, the method of characteristics (MOC) is the most popular one due to its accuracy, simplicity and ability to include different boundary conditions in the one dimensional case [4]. This method has also been adapted for two dimensional cases to account for the frequency dependence of the friction forces [5, 6] and extended to be

applied in more complex hydraulic networks, [7, 8]. However, the MOC together with other discrete formulations such as finite differences [9], require a spatial discretization of the lines in the network, which turns to be computationally demanding as discussed in [10].

For laminar flow, another approach to model the fluid transients is possible through modal approximations. The idea behind this technique is to represent the transcendental expressions in the frequency domain, as a finite summation of low-order polynomial transfer functions. Thus, it is possible to approximate each mode of the transmission line by a second order linear differential equation [11–14]. The modal method can also be formulated directly in the time domain using a variational method [15]. The modal approximation has certain advantages when used in time domain simulations, not only because it is easily coupled to other mechanical or hydraulic subsystems, but additionally because it can be implemented and solved numerically with a variable time step ODE solver. Furthermore, several studies have shown that modal methods are more convenient and numerically stable when compared, for example, with discrete methods [16, 17]. On the contrary, when modal approximations are used to construct hydraulic networks as a part of a complex fluid power system, i.e. through bond-graph models [18, 19], each line in the network should include enough number of modes to cover the frequency range of interest of both the overall system and input disturbance. Due to the different line geometries and interface conditions, the selection of the required number of modes for each line is not straightforward. Therefore, the modal method has the disadvantage of lacking a direct control on the accuracy of the results due to a propagation error introduced by the number of modes used for each line.

A semi-analytical approach is presented in this paper based on the impulse response method (IRM). This method has been extensively used for dynamic analyses in other areas, like for example vibrations of mechanical systems, however its use in hydraulic systems has not been completely exploited. A variation of this method has already been used for analysis of a single pipeline as referred in [20, 21]. This work presents a direct extension towards a solution of a hydraulic network system consisting of multiple lines including dissipative boundary conditions. The approach is remarkably simple in its application. It consists of a solution of a coupled system of linear algebraic equations and the use of the Fourier transform. The method is accurate and reliable for the solution of large networks, overcoming the disadvantages of several other approaches.

The paper is composed as follows. Section 2 revises the mathematical formulation of the two dimensional viscous compressible model for a single pipeline together with the exact

solution of a hydraulic network in the frequency domain. Section 3 describes the application of the impulse response method to solve a hydraulic network using the equations of the previous section. In section 4, a numerical example of a simple hydraulic network is presented in which the time-domain results are compared with the ones obtained by the use of the modal method. Finally the conclusions are presented in the last section.

## 2 Mathematical formulation and exact solution in the frequency domain

### 2.1 Transient laminar flow

Consider a laminar, axisymmetric flow of a Newtonian fluid through a constant diameter line with constant material properties, in which the mean fluid velocity is considerably less than the acoustic velocity and the thermodynamic effects are neglected. The velocities in the axial  $x$ -coordinate and radial  $r$ -coordinate are denoted by  $u(x, r, t)$  and  $v(x, r, t)$ , respectively. Assuming that the motion in the radial direction is negligible compared to the motion in the axial direction  $u \gg v$ , the radial pressure distribution is constant across the cross-sectional area, i.e.  $P(x, t)$ .

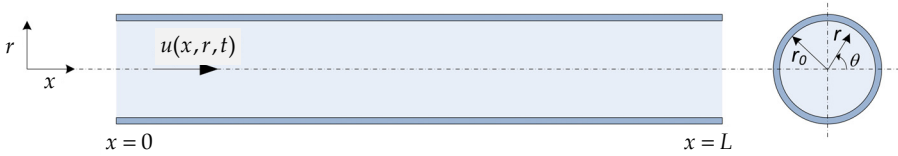


Figure 1. Schematic of a single hydraulic line

The fluid properties are designated through the fluid density  $\rho$ , the fluid dynamic viscosity  $\mu$  and the fluid bulk modulus of elasticity  $K$ . Hence, the partial differential equations corresponding to the mass conservation and the momentum equilibrium in the axial direction, are reduced to [1],

$$\frac{\partial P(x, t)}{\partial t} + c^2 \rho \left[ \frac{\partial u(x, r, t)}{\partial x} + \frac{\partial v(x, r, t)}{\partial r} + \frac{v(x, r, t)}{r} \right] = 0 \quad (1)$$

$$\frac{\partial u(x, r, t)}{\partial t} + \frac{1}{\rho} \frac{\partial P(x, t)}{\partial x} = \mu \left[ \frac{\partial^2 u(x, r, t)}{\partial r^2} + \frac{1}{r} \frac{\partial u(x, r, t)}{\partial r} \right] \quad (2)$$

where the effective speed of sound in the fluid is  $c = \sqrt{K_e / \rho}$ ; the effective bulk modulus of the fluid  $K_e$  takes into account the flexibility of the pipeline, compressibility of the hydraulic fluid and the effect of any entrapped air into the system.

The cross-sectional volumetric flow is obtained through the integration of the axial velocity across the cross-sectional area of the line with finite radius  $r_0$ . The volumetric flow is also defined as the product of the average velocity  $\bar{u}(x, t)$  and the cross-sectional area.

$$Q(x, t) = \pi r_0^2 \bar{u}(x, t) = \int_0^{r_0} u(x, r, t) 2\pi r dr \quad (3)$$

The previous equations correspond to what is known as a two-dimensional viscous compressible model or dissipative friction model [2, 3].

## 2.2 General solution of a single line

The general solution of equations 1 and 2 can be obtained in the frequency domain by using the Fourier transform with respect to time according to the following transformation pair,

$$\tilde{f}(\omega) = \int_{-\infty}^{\infty} f(t) e^{-j\omega t} dt \quad (4)$$

$$f(t) = \frac{1}{2\pi} \int_{-\infty}^{\infty} \tilde{f}(\omega) e^{j\omega t} d\omega \quad (5)$$

here  $\omega$  represents the frequency and  $j = \sqrt{-1}$  is a complex value. The average velocity and the pressure are then given by the following two equations [1],

$$\bar{U}(x, \omega) = \left[ A(\omega) \cos \frac{j\omega\beta}{c} x + B(\omega) \sin \frac{j\omega\beta}{c} x \right] \frac{1}{\beta^2} J_0 \left[ j \sqrt{\frac{j\omega r_0^2}{\nu}} \right] \quad (6)$$

$$\bar{P}(x, \omega) = \left[ A(\omega) \sin \frac{j\omega\beta}{c} x - B(\omega) \cos \frac{j\omega\beta}{c} x \right] \frac{\rho c}{\beta} J_0 \left[ j \sqrt{\frac{j\omega r_0^2}{\nu}} \right] \quad (7)$$

in which  $A(\omega)$  and  $B(\omega)$  are the unknown integration constants to be obtained from the applied boundary conditions;  $\nu = \mu / \rho$  is the kinematic viscosity of the fluid and the constant  $\beta$  is expressed through the Bessel functions of the first kind  $J_n(z)$  with  $n = 0, 1$ .

$$\beta = \left( \frac{2}{j\sqrt{\frac{j\omega r_0^2}{v}}} \frac{J_1 \left[ j\sqrt{\frac{j\omega r_0^2}{v}} \right]}{J_0 \left[ j\sqrt{\frac{j\omega r_0^2}{v}} \right]} - 1 \right)^{\frac{1}{2}} \quad (8)$$

Using the boundary conditions at the upstream section where  $x = 0$ , and at the downstream section with  $x = L$ , the integration constants  $A(\omega)$  and  $B(\omega)$  are obtained for a single pipeline. Hence the velocity and pressure at the upstream side  $\bar{U}_u(\omega)$ ,  $\bar{P}_u(\omega)$  can be expressed in terms of the downstream velocity and pressure  $\bar{U}_d(\omega)$ ,  $\bar{P}_d(\omega)$ . If the volumetric flow is used instead of the average velocity using equation 3, the following relations are formulated in matrix form,

$$\begin{bmatrix} P_u(\omega) \\ Q_u(\omega) \end{bmatrix} = \begin{bmatrix} \cos \frac{j\omega\beta L}{c} & -\frac{\beta\rho c}{\pi r_0^2} \sin \frac{j\omega\beta L}{c} \\ \frac{\pi r_0^2}{\beta\rho c} \sin \frac{j\omega\beta L}{c} & \cos \frac{j\omega\beta L}{c} \end{bmatrix} \begin{bmatrix} P_d(\omega) \\ Q_d(\omega) \end{bmatrix} \quad (9)$$

A most common representation of the previous equation is done in terms of hyperbolic functions instead of trigonometric functions. The hyperbolic notation is a popular way to show the solution for a single line and its derivation is found in the Appendix.

Two pipeline parameters are introduced, the line impedance constant  $Z_0$  and the dissipation number of the line  $D_n$  are defined respectively as:

$$Z_0 = \frac{\rho c}{\pi r_0^2} \quad (10)$$

$$D_n = \frac{vL}{r_0^2 c} \quad (11)$$

### 2.3 Extension towards the solution of a hydraulic network

The solution of a complete hydraulic network consisting of multiple lines is an extension of the solution given by equations 6 and 7. Using equation 3, a general solution for the flow and pressure of each of the lines of the network, denoted by the subscript  $i$ , is given by:

$$Q_i(x, \omega) = \left[ A_i(\omega) \cos \frac{j\omega\beta_i}{c} x + B_i(\omega) \sin \frac{j\omega\beta_i}{c} x \right] \frac{\rho c}{Z_{0,i} \beta_i^2} J_0 \left[ j\sqrt{\frac{j\omega r_{0,i}^2}{v}} \right] \quad (12)$$

$$P_i(x, \omega) = \left[ A_i(\omega) \sin \frac{j\omega\beta_i}{c} x - B_i(\omega) \cos \frac{j\omega\beta_i}{c} x \right] \frac{\rho c}{\beta_i} J_0 \left[ j \sqrt{\frac{j\omega r_{0,i}^2}{\nu}} \right] \quad (13)$$

The difference from the solution for a single pipeline is that the integrations constants for the pressure and flow descriptions cannot be determined explicitly for each of the lines of the hydraulic network. Instead they are obtained numerically by solving a linear system of coupled equations compiled from the various boundary and interface conditions according to the particular configuration of the system. The system of equations written in matrix form is

$$\mathbf{A}\bar{x} = \bar{b} \quad (14)$$

where  $\mathbf{A}$  is the global system matrix, whose elements are frequency dependent. The vector  $\bar{x}$  corresponds to the unknown integration constants for the network consisting of  $n$  lines.

$$\bar{x} = [A_1(\omega), B_1(\omega), A_2(\omega), B_2(\omega), \dots, A_n(\omega), B_n(\omega)]^T \quad (15)$$

The right-hand side vector  $\bar{b}$  corresponds to the external forcing terms at the boundary conditions or interfaces. Thus, the solution of a complex network is only limited by the computational considerations to solve a system of algebraic linear equations. The order of this system of equations is twice the number of lines in the hydraulic network,  $2n$ .

#### 2.4 Interface and boundary conditions

The interface conditions correspond to the junction points or nodes in systems of branching pipes. At these particular locations, the continuity equation is used to relate the inflows and outflows of the discharges at each node or junction, see equation 16. In addition, another set of equations is obtained through the general assumption of uniqueness of the pressure at each junction or node  $k$  according to equation 17.

$$\sum Q_{in}(x_k, \omega) - \sum Q_{out}(x_k, \omega) = 0 \quad (16)$$

$$P^l(x_k, \omega) = P^r(x_k, \omega) \quad (17)$$

The different boundary conditions at the terminations of the lines could include any linear static or dynamic hydraulic component. An example of a static boundary condition is a resistive component, which relates the volumetric flow with the pressure difference across

the element at each moment of time through the hydraulic resistance  $R$ ; in the frequency domain this condition is given by,

$$P_a(\omega) - P_b(\omega) - RQ_b(\omega) = 0 \quad (18)$$

A dynamic termination as a boundary condition is also possible, (i.e. a line termination with a large volume of fluid or an actuator). For this example the relation is given through a first order linear differential equation for the pressure  $P_b$ , where the hydraulic capacitance  $C_1$  accounts for the fluid compressibility. The representation in both time and frequency domain is given as,

$$C_1 \frac{dP_b(t)}{dt} - Q_b(t) = 0 \quad (19)$$

$$C_1 j\omega P_b(\omega) - Q_b(\omega) = 0 \quad (20)$$

The treatment of a non-linear boundary condition at one of the terminations is also possible through this method; in this case a simultaneous numerical solution of the non-linear boundary condition equation and the convolution integral at the boundary is required. An example is shown in [20], for the particular case of a non-linear valve description.

### 3 Impulse response method for hydraulic networks

The impulse response method makes use of the superposition property of linear systems; if an arbitrary but known input is decomposed to a series of impulses of different amplitudes, the response of the system is obtained by the superposition of the responses of each impulse. Thus, if the system or hydraulic network pressure and/or flow response to an impulse is known in the time domain, its response to a general forcing function can be obtained through the convolution of the impulse response and the forcing function.

A known input at one of the boundaries of the hydraulic network can be given as either a pressure function  $\Delta P(t)$  or flow function  $\Delta Q(t)$ . The pressure response of the system at a given location  $P(x, t)$  is therefore provided by the convolution of the pressure response at the same location to a pressure impulse  $r_{Px}(t)$  and the desired pressure input function  $\Delta P(t)$

$$P(x, t) = \int_0^t r_{Px}(t - \tau) \Delta P(\tau) d\tau \quad (21)$$

in which  $t$  is a time variable used for the convolution. Or in the case of a flow input  $\Delta Q(t)$  the convolution uses the pressure response to a flow impulse  $r_{Qx}(t)$  and the flow input function,

$$P(x, t) = \int_0^t r_{Qx}(t - \tau) \Delta Q(\tau) d\tau \quad (22)$$

Hence, in order to obtain the system response to an impulse, the complete hydraulic network is first solved in the frequency domain  $r_x(\omega)$ . Afterwards, the inverse Fourier transform of the pressure and/or flow is applied at the desired locations to obtain the time domain description  $r_x(t)$ .

$$r_x(t) = \frac{1}{2\pi} \int_{-\infty}^{\infty} r_x(\omega) e^{j\omega t} d\omega = \frac{1}{\pi} \operatorname{Re} \left[ \int_0^{\infty} r_x(\omega) e^{j\omega t} d\omega \right] \quad (23)$$

An efficient way to obtain such response from a numerical perspective, is to use the discrete fast Fourier transform (FFT). Although the FFT is based on a fixed discrete time step, the impulse response has only to be calculated once for the whole network. Once this response is available for the particular configuration, the numerical convolution is obtained in a separate step for any desired input without the necessity to solve the system once more. Furthermore the convolution can also be implemented for a variable step approach.

### 3.1 Computational efficiency comparison

For large hydraulic networks, the computational efficiency of the proposed method can be compared with other approaches. A general overview is observed in table 1. Hence let us consider a network comprising of  $n_{\text{lines}} = 100$ . In the MOC, first of all an internal discretization is required; assuming that ten elements are used per line, a final grid of around 1,000 points is obtained. Every time step, a solution using finite differences is found for all the points in the grid. With the modal method no discretization is required, however a few modes are needed at least to model each line  $n_{\text{modesperline}} = 4$ . Assuming that four modes are used to describe accurately each line, a system of 900 ode's is obtained. It is important to mention that the order of the final system might be considerably higher as the number of modes per line is independent and some lines would require higher modes in order to obtain a minimum accuracy. Finally the IRM requires the solution of an independent linear system of equations of  $200 \times 200$  per frequency (which is equivalent as



per time step in the frequency domain), where the obtained solution is exact. At the end of the method, an inverse FFT is required but the computational cost of this operation is also independent of the number of lines in the network.

Table 1: Overview of calculation requirements for hydraulic networks

| Approach     | Calculation requirements per $\Delta t$  |
|--------------|--|
| MOC          | Solution required at all interior points of the grid; results are approximate.   |
| Modal method | Solution to a system of linear ordinary differential equations $n_{\text{lines}}(4n_{\text{modesperline}} + 1)$ ; results are approximate.   |
| IRM          | Solution to a system of linear algebraic equations $2n_{\text{lines}} \times 2n_{\text{lines}}$ ; exact results in frequency domain, accuracy in time domain depends on FFT required at the end of the method. |

#### 4 Numerical results

In order to illustrate the proposed method and to compare the predictions with the modal approach proposed in the literature [18], three cases are solved numerically based on the simple hydraulic network shown in figure 2. The forcing input function  $\Delta P(t)$  is a unit step pressure at the upstream side  $x = 0$ . The examples include different linear terminations and the input parameters for each case are summarized in table 2. It is important to note that the dissipation numbers of each line are relatively high  $D_n \gg 0.0001$ .  $D_n$  is a dimensional number which is used to characterize both transient and frequency response of a pipeline and given by equation 11; a high value implies that the energy dissipation

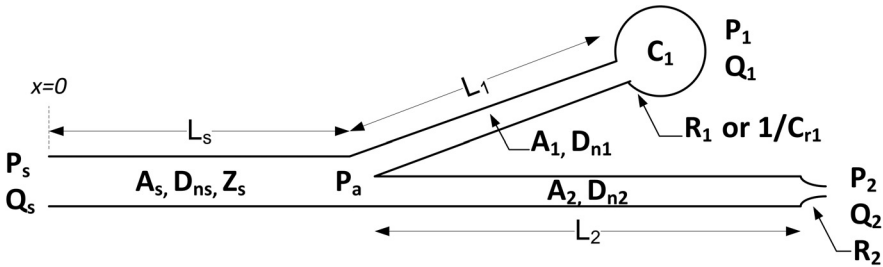


Figure 2. Schematic of the hydraulic network used for the numerical simulations

due to the shear friction at the wall of the line is important. Therefore the dissipative model with frequency-dependent friction will give a more accurate description of the transient behaviour than the linear friction model.

In general, there exist two unknown integration constants for each line comprising the network. This means that for the particular configuration shown in figure 2, six independent linear equations are required. The first equation corresponds to the boundary condition at the upstream side of the supply line where the required pressure impulse is applied at  $x = 0$ . Three more equations are obtained from the interface conditions at the branching node  $a$ ; one for the continuation of flows; the other two from the uniqueness assumption of the pressure. The supply line of the network is noted by the subscript  $s$ , while the two other branch lines are noted by the subscripts 1 and 2 respectively.

$$\text{at } x = 0 \quad P_s(0, \omega) = 1 \quad (24)$$

$$\text{at } x = L_s \quad Q_s(L_s, \omega) - Q_1(L_s, \omega) - Q_2(L_s, \omega) = 0 \quad (25)$$

$$P_s(L_s, \omega) - P_1(L_s, \omega) = 0 \quad (26)$$

$$P_s(L_s, \omega) - P_2(L_s, \omega) = 0 \quad (27)$$

The fifth and sixth equations are derived from the boundary conditions at the terminations of the hydraulic lines 1 and 2. Once the integration constants are obtained for all the lines in the network, the average velocity and pressure can be evaluated at any desired location by equations 12 and 13. The time domain response of the pressure impulse is obtained numerically through the discrete inverse FFT. For all cases, the number of samples used was  $N = 2^{16}$ , with a discrete step time of 0.0001 s. The selected time step allows to follow the pressure wave propagation along the spatial coordinate with sufficient detail.

Furthermore, it includes frequency components up to 5000 Hz which are sufficient to

Table 2. Numerical parameters for the different cases taken from [18]

|        | $D_{ns}$ | $D_{n1}$ | $D_{n2}$ | $\frac{L_1}{L_s}$ | $\frac{L_2}{L_s}$ | $\frac{A_1}{A_s}$ | $\frac{A_2}{A_s}$ | $\frac{R_1}{Z_s}$ | $\frac{R_2}{Z_s}$ | $\frac{C_1}{C_c} *$ |
|--------|----------|----------|----------|-------------------|-------------------|-------------------|-------------------|-------------------|-------------------|---------------------|
| Case 1 | 0.1      | 0.1      | 0.1      | 1                 | 1                 | 1                 | 1                 | $\infty$          | 3                 | -                   |
| Case 2 | 0.01     | 0.01     | 0.1      | 1                 | 5                 | 1                 | 0.5               | $\infty$          | $\infty$          | -                   |
| Case 3 | 0.01     | 0.1      | 0.1      | 5                 | 10                | 0.5               | 1                 | 2                 | 6                 | 0.25                |

\* with  $C_c = \frac{\pi L_s r_s^2}{\rho c^2}$

describe the step input considered in the examples. The final step is to convolute numerically the impulse response with a step function to obtain the desired step response of the system in the time domain.

#### 4.1 Model comparison and discussion

The results for each case are compared with the results of the same network using the modal method. The modal method is based on four modes for each of the lines in the hydraulic network as presented in [18].

##### Case 1

All the lines have the same geometric characteristics; one of the terminations of the pipeline is blocked while the other consist of a linear resistance element; the boundary conditions are shown in equations 28 and 29.

$$\text{at } x = L_1 \quad Q_1(L_1, \omega) = 0 \quad (28)$$

$$\text{at } x = L_2 \quad P_2(L_2, \omega) - R_2 Q_2(L_2, \omega) = 0 \quad (29)$$

The pressure response to an impulse at the locations  $P_a, P_1, P_2$  is shown in figure 3a; this response is numerically convoluted with a unit step input to obtain the results of figure 3b. Figure 3c shows the comparison of results with the modal method. The pressure transient shows a smooth response which is accurately described, with minor differences, by both methods. However, the modal method contains spurious oscillations at the initial moments in time, which are not present in the results of the IRM. The oscillations present in the modal method are impossible to eliminate since this would require the inclusion of infinitely many modes. In the presented method such oscillations are absent since the solution is exact.

##### Case 2

In this case, different geometries of the lines are used and both terminations are blocked; the respective boundary conditions are given in equations 30 and 31.

$$\text{at } x = L_1 \quad Q_1(L_1, \omega) = 0 \quad (30)$$

$$\text{at } x = L_2 \quad Q_2(L_2, \omega) = 0 \quad (31)$$

As seen in figure 4, when blocked terminations are used, the modal approximations are inadequate to provide an accurate response of the system. Spurious oscillations are again

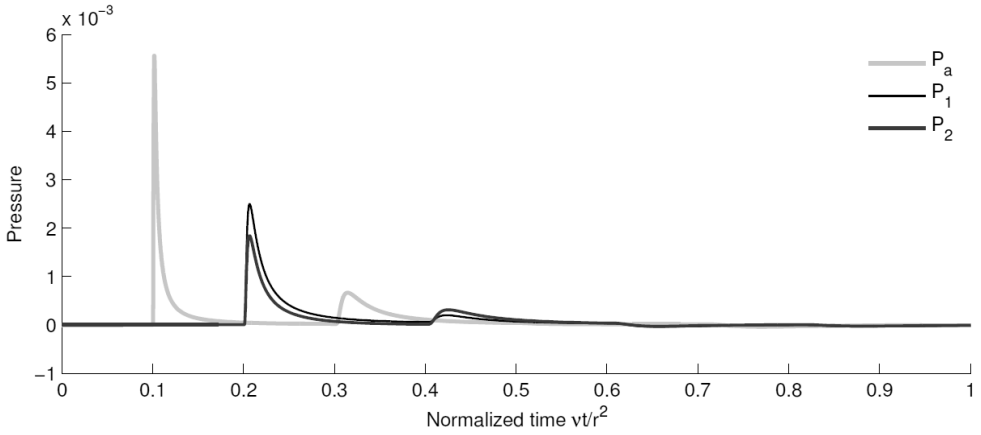


Figure 3a. Impulse response comparison of case 1

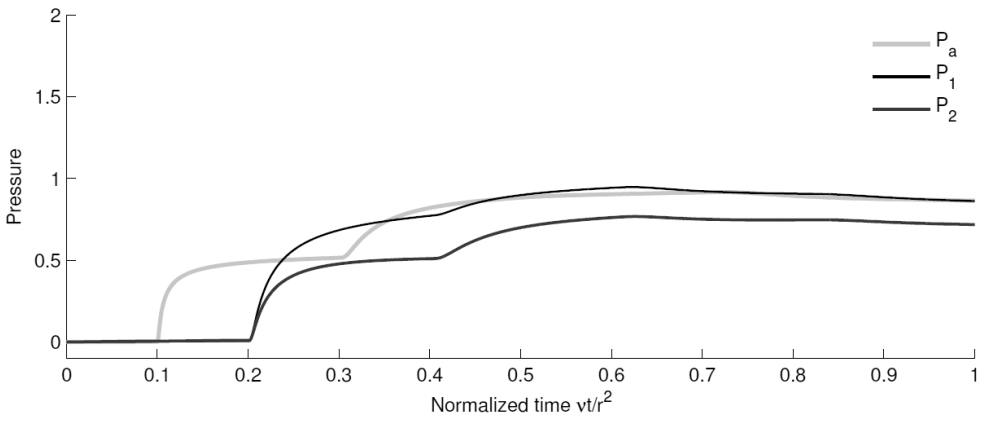


Figure 3b. Step response comparison of case 1

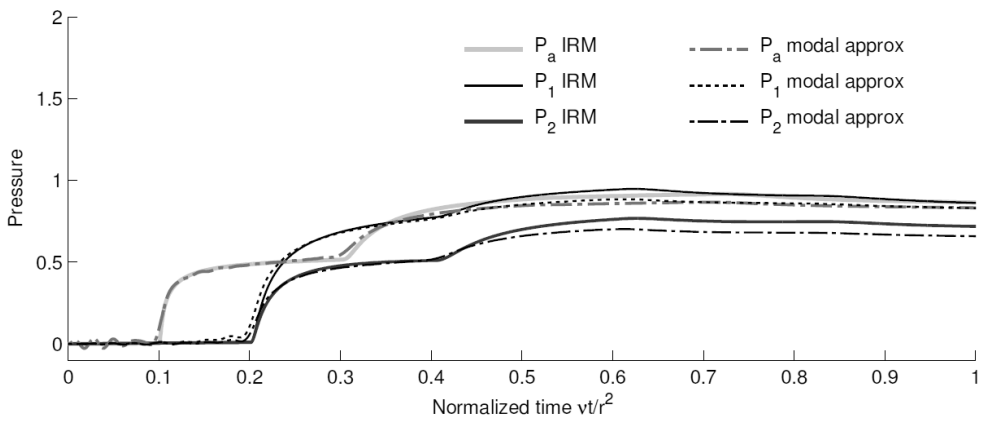


Figure 3c. Step response comparison between the IRM and modal approximations of case 1

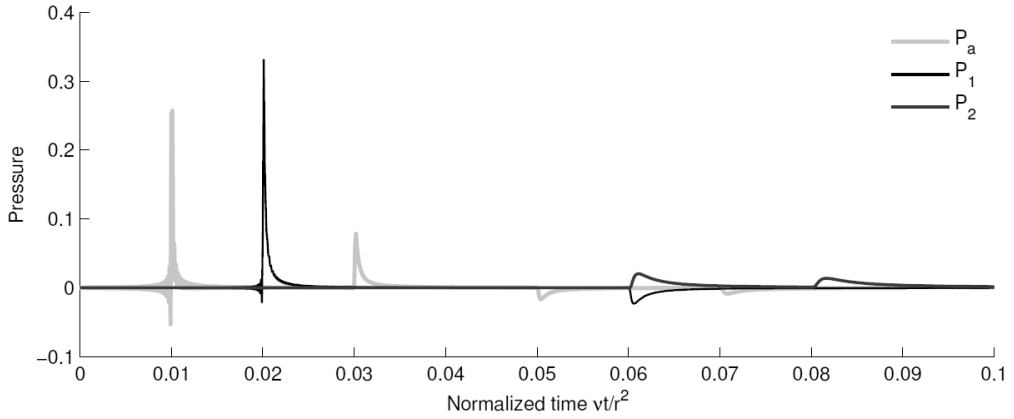


Figure 4a. Impulse response comparison of case 2

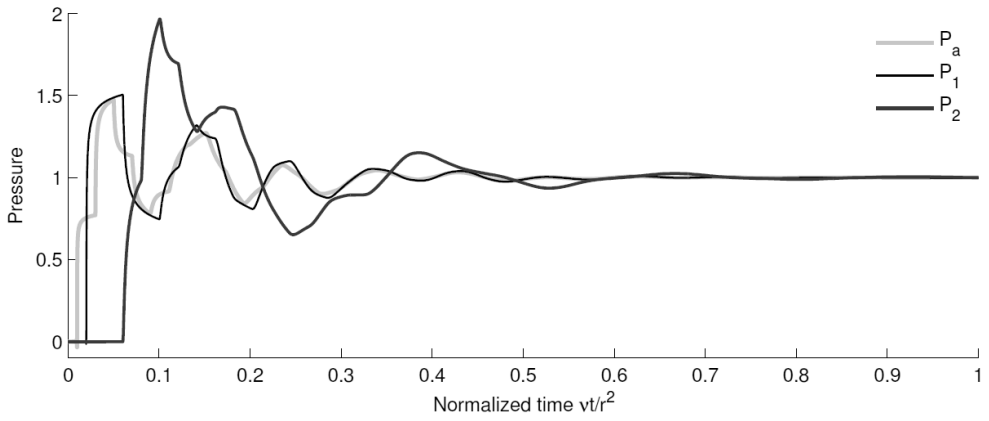


Figure 4b. Step response comparison of case 2

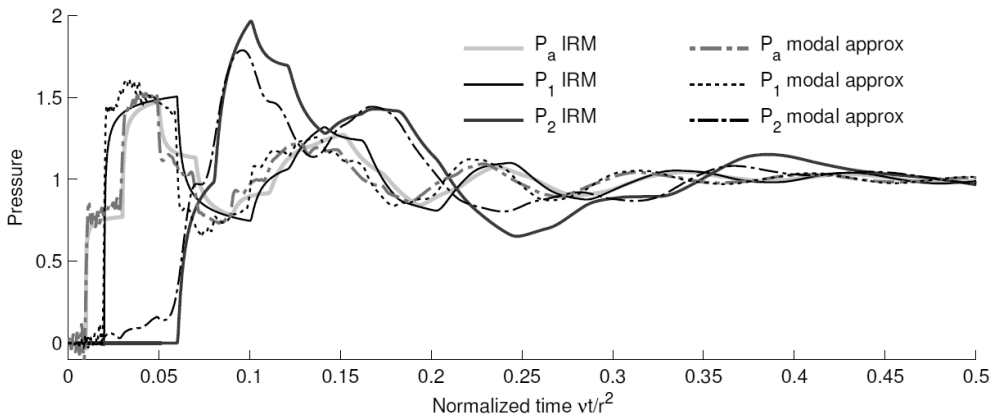


Figure 4c. Step response comparison between the IRM and modal approximations of case 2

present at the initial moments of time for the reason explained previously. In addition, a higher dissipation of the transient response is observed in the modal approximations together with a phase difference.

The results provided by the IRM method also show sharp variations in the pressure response due to reflected wave fronts, however this effect is not captured correctly by the modal method.

### Case 3

In the final case 3, different geometries are present with both dynamic and static terminations, such boundaries are given through equations 32 and 33.

$$\text{at } x = L_1 \quad P_1(L_1, \omega) - \left( \frac{1}{C_1 j \omega} + R_1 \right) Q_1(L_1, \omega) = 0 \quad (32)$$

$$\text{at } x = L_2 \quad P_2(L_2, \omega) - R_2 Q_2(L_2, \omega) = 0 \quad (33)$$

In figure 5 the results show a relatively smooth response for both methods. As can be seen, the pressure response  $P_a$  at the hydraulic branch using modal approximations, presents large oscillations specially after the first wave front surpasses the branch junction. The oscillations might be reduced by increasing the number of modes for this particular line. Hence, it is evident that even for a relatively simple network the modal method has not direct control in the required number of modes for each line.

From the results presented in the previous cases, it is clear that sharp wave fronts and reflections cannot be approximated with a few number of modes. For larger networks with multiple number of lines, the inclusion of a large number of modes per line can be both computationally demanding and inexact. On the contrary, the adopted IRM method is based on an exact solution in the frequency domain, making this approach more accurate and reliable for the solution of larger networks, overcoming the disadvantages of several other approaches.

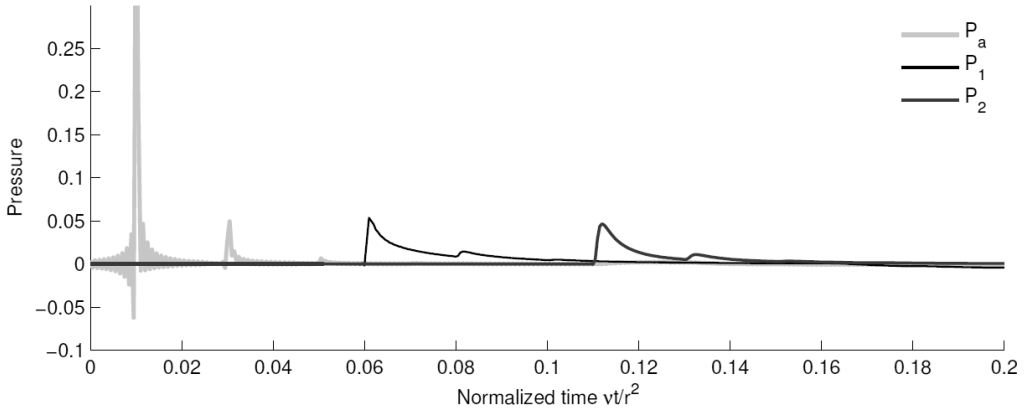


Figure 5a. Impulse response comparison of case 3

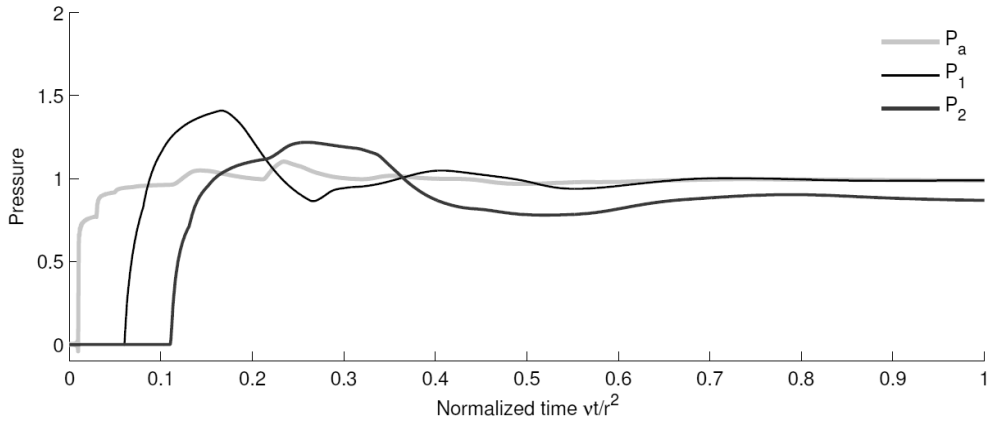


Figure 5b. Step response comparison of case 3

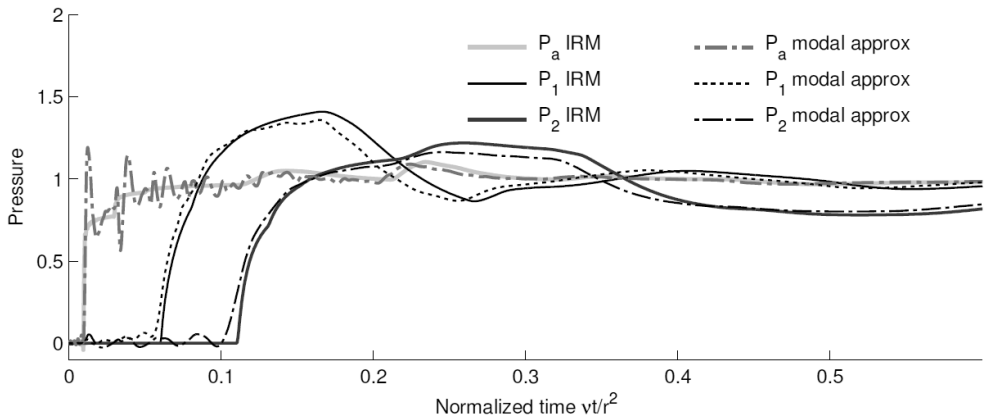


Figure 5c. Step response comparison between the IRM and modal approximations of case 3

## 5 Conclusions

An application of a semi-analytical impulse response method to hydraulic networks was presented for transient laminar flow using a two-dimensional viscous compressible model. By solving analytically the complete network in the frequency domain, a unique impulse response of pressure and/or volumetric flow is obtained in the time-domain through the inverse FFT. A discrete numerical convolution with respect to time is then applied separately to obtain the response of the complete network to a chosen arbitrary input. Although the application of the method was shown for a simple hydraulic network, it can be easily extended to networks with large numbers of lines with various interface and boundary conditions.

Since the IRM does not require any spatial discretization, it is expected that the computational cost has a great advantage, especially for applications in large networks, when compared to existing grid-space methods. The method is only limited by the numerical considerations to solve a system of coupled linear algebraic equations and the fast Fourier transform. This means that for large networks, the increase in computational cost is only determined by the order of the global system matrix, which is linearly dependent to the number of lines forming the system.

In addition, the presented results show that the adopted IRM method provides a more accurate description of the transient behaviour than the modal approximation of individual lines used for network modelling. For a large network, the modal method might provide inaccurate results, as the required number of modes for each line is not *a priori* known.

## References

- [1] D'Souza A.F., Oldenburger R., 1964, "Dynamic Response of Fluid Lines," *J. Basic Eng.*, **86**, pp. 589-598.
- [2] Goodson R.E., Leonard R.G., 1972, "A Survey of Modeling Techniques for Fluid Line Transients," *J. Basic Eng.*, **94**, pp. 474-482.
- [3] Stecki J., Davis D., 1986, "Fluid Transmission Lines-Distributed Parameter Models, Part 1: A Review of the State of the Art," *Proc. Inst. Mech. Eng., Part A*, **200**, pp. 215-228.
- [4] Wylie E., Streeter V., Suo L., 1993, *Fluid Transients in Systems*, Prentice-Hall.



- [5] Zielke W., 1968, "Frequency-Dependent Friction in Transient Pipe Flow," *J. Basic Eng.*, **90**, pp. 109-115.
- [6] Trikha A.K., 1975, "An Efficient Method for Simulating Frequency- Dependent Friction in Transient Liquid Flow," *ASME Trans. J. Fluids Eng.*, **97**, pp. 97-105.
- [7] Karney B. W., McInnis D., 1992, "Efficient calculation of transient flow in simple pipe networks," *J. Hyd. Eng.*, **118** (7), pp. 1014-1030.
- [8] Wichowski R., 2006, "Hydraulic transients analysis in pipe networks by the method of characteristics (MOC)," *Archives of Hydro-Engineering and Environmental Mechanics*, **53** (3), pp. 267-291.
- [9] Pezzinga G., 1999, "Quasi-2D model for unsteady flow in pipe networks," *J. Hyd. Eng.*, **125** (7), pp. 676-685. 12
- [10] Wood D.J., Lingireddy S., Boulos P.F., Karney B.W., McPherson D.L., 2005, "Numerical methods for modeling transient flow in distribution systems," *Journal American Water Works Association*, **97** (7), pp. 104-115.
- [11] Hsue C.Y., Hullender D.A., 1983, "Modal Approximations for the Fluid Dynamics of Hydraulic and Pneumatic Transmission Lines," *Fluid Transmission Line Dynamics*, M. E. Franke and T. M. Drzewiecki, eds., ASME Special Publication, New York, pp. 51-77.
- [12] Yang W. C., Tobler W. E., 1991, "Dissipative Modal Approximation of Fluid Transmission Lines Using Linear Friction Model" *J. Dyn. Syst. Meas. Control*, **113**, pp. 152-162.
- [13] Van Schothorst G., 1997, "Modeling of Long-Stroke Hydraulic Servo-Systems for Flight Simulator Motion Control and System Design," Ph.D. thesis, Delft University of Technology, The Netherlands.
- [14] Ayalew B., Kulakowski B.T., 2005, "Modal Approximation of Distributed Dynamics for a Hydraulic Transmission Line With Pressure Input-Flow Rate Output Causality," *J. Dyn. Syst. Meas. Control*, **127**, pp. 503-507.
- [15] Mäkinen J., Piche R., Ellman A., 2000, "Fluid Transmission Line Modeling Using a Variable Method," *J. Dyn. Syst. Meas. Control*, **122**, pp. 153-162.
- [16] Watton J., Tadmori M., 1988, "A Comparison of Techniques for the Analysis of Transmission Line Dynamics in Electrohydraulic Control Systems," *Appl. Math. Modelling*, **12**, pp. 457-466.
- [17] Soumelidis M.I., Johnston D.N., Edge K.A., Tilley D.G., 2005, "A Comparative Study of Modelling Techniques for Laminar Flow Transients in Hydraulic Pipelines," JFPS conf.
- [18] Margolis D. L., and Yang W. C., 1985, "Bond Graph Models for Fluid Networks Using Modal Approximation," *J. Dyn. Syst. Meas. Control*, **107**, pp. 169-175.

- [19] Yang L., Hals J., Moan T., 2012, "Comparative study of bond graph models of hydraulic transmission lines with transient flow dynamics," *J. Dyn. Syst. Meas. Control*, **134**, 031005.
- [20] Suo Lisheng, Wylie E.B., 1989, "Impulse response method for frequency dependent pipeline transients," *ASME Trans. J. Fluids Eng.*, **111**, pp. 478-483.
- [21] Kim S., 2011, "Holistic unsteady-friction model for laminar transient flow in pipeline systems" *J. Hyd. Eng.*, **137** (12), pp. 1649-1658.

## Appendix

The matrix solution for a single line can also be expressed in terms of the complex Laplace variable  $s = \sigma + j\omega$ ; where  $\sigma$  is a decay factor and  $\omega$  represents the frequency. Hence, equation 9 is rewritten as,

$$\begin{bmatrix} P_u(s) \\ Q_u(s) \end{bmatrix} = \begin{bmatrix} \cos \frac{s\beta L}{c} & -\frac{\beta \rho c}{\pi r_0^2} \sin \frac{s\beta L}{c} \\ \frac{\pi r_0^2}{\beta \rho c} \sin \frac{s\beta L}{c} & \cos \frac{s\beta L}{c} \end{bmatrix} \begin{bmatrix} P_d(s) \\ Q_d(s) \end{bmatrix} \quad (34)$$

The previous equation can also be expressed in terms of hyperbolic functions instead of trigonometric function using the relations  $\sin jx = j \sinh x$  and  $\cos jx = \cosh x$ . The hyperbolic notation is the most usual way to show the solution for a single line as it is expressed only in terms of the line characteristic impedance  $Z_c(s)$  and the propagation operator  $\Gamma(s)$  [2, 3].

$$\begin{bmatrix} P_u(s) \\ Q_u(s) \end{bmatrix} = \begin{bmatrix} \cosh \Gamma(s) & Z_c(s) \sinh \Gamma(s) \\ \frac{1}{Z_c(s)} \sinh \Gamma(s) & \cosh \Gamma(s) \end{bmatrix} \begin{bmatrix} P_d(s) \\ Q_d(s) \end{bmatrix} \quad (35)$$

This general notation allows to use the solution for the different distributed parameters models (i.e. 1D inviscid model, 1D linear friction model) depending on the expression used for the terms  $Z_c(s)$  and  $\Gamma(s)$ . Using the normalized Laplace operator  $\bar{s} = s / \omega_c$ , where  $\omega_c = \nu / r_0^2$  is the viscosity frequency, the line characteristic impedance  $Z_c(\bar{s})$  and the propagation operator  $\Gamma(\bar{s})$  are given by,

$$Z_c(\bar{s}) = Z_0 \left[ 1 - \frac{2}{j\sqrt{\bar{s}}} \frac{J_1[j\sqrt{\bar{s}}]}{J_0[j\sqrt{\bar{s}}]} \right]^{-\frac{1}{2}} \quad (36)$$

$$\Gamma(\bar{s}) = D_n \bar{s} \left( 1 - \frac{2}{j\sqrt{\bar{s}}} \frac{J_1[j\sqrt{\bar{s}}]}{J_0[j\sqrt{\bar{s}}]} \right)^{-\frac{1}{2}} \quad (37)$$

